Synthesis of lignin-functionalized phenolic nanospheres supported Ag nanoparticles with excellent dispersion stability and catalytic performance

Shilin Chen,[a] Guanhua Wang,[a]* Wenjie Sui,[b] Ashak Mahmud Parvez [c] and Chuanling Si [a]*

[a] Tianjin Key Laboratory of Pulp and Paper, College of Light Industry Science and Engineering, Tianjin University of Science and Technology, Tianjin 300457, China

[b] State Key Laboratory of Food Nutrition and Safety, Tianjin University of Science and Technology, Tianjin 300457, China

[c] Department of Mechanical Engineering, University of New Brunswick, Fredericton, NB, E3B 5A3, Canada

* Corresponding author. Tel.: +86 02260601313

Address: No.29 at 13th Avenue, TEDA, Tianjin 300457, China

E-mail address: ghwang@tust.edu.cn (Guanhua Wang)

sichli@tust.edu.cn (Chuanling Si)

Experiment sections

Preparation of lignin-based phenolic resin (LPR) spheres with different lignin addition ratios

The formula of reagents for LPR spheres fabrication with different lignin addition ratios (replacement ratios of phenol by lignin) are presented in Table 1S. The reagents including lignin, phenol, formaldehyde, and NaOH were weighted based on the formula and mixed sufficiently in aqueous ethanol solution (20 mL of deionized water and 8 mL of ethanol). The mixture solution was then heated at 65 ^{o}C for 1 h and 90 ^{o}C for 30 min, respectively. Afterward, the mixture solution was transferred into a sealed Teflon-lined stainless steel autoclave and heated at 120 ^{o}C for 12 h, followed by natural cooling to room temperature. The solid products were collected by centrifugation (10000 rpm, 5 min), and washed using deionized water and ethanol three times, respectively. Finally, the thermosetting LPR spheres with different lignin addition ratios were obtained by vacuum drying at 80 ^{o}C for 12 h.

Table S1. Formula for lignin-based phenolic resin preparation with different lignin addition ratios

Addition ratios (R, %)	Lignin (g)	Phenol (g)	37% aqueous formaldehyde (g)	NaOH (g)
0	0	0.2	0.28	0.0170
5	0.01	0.19	0.27	0.0172
10	0.02	0.18	0.26	0.0173
20	0.04	0.16	0.23	0.0176
40	0.08	0.12	0.19	0.0182
50	0.1	0.1	0.17	0.0185

The lignin addition ratio was calculated according to the replacement ratios *R*.

$$R=L/(L+P)\times 100\% \qquad (1)$$

Where *R* was the adition ratio of lignin, *L* was the mass of lignin added and *P* was the mass of phenol [1].

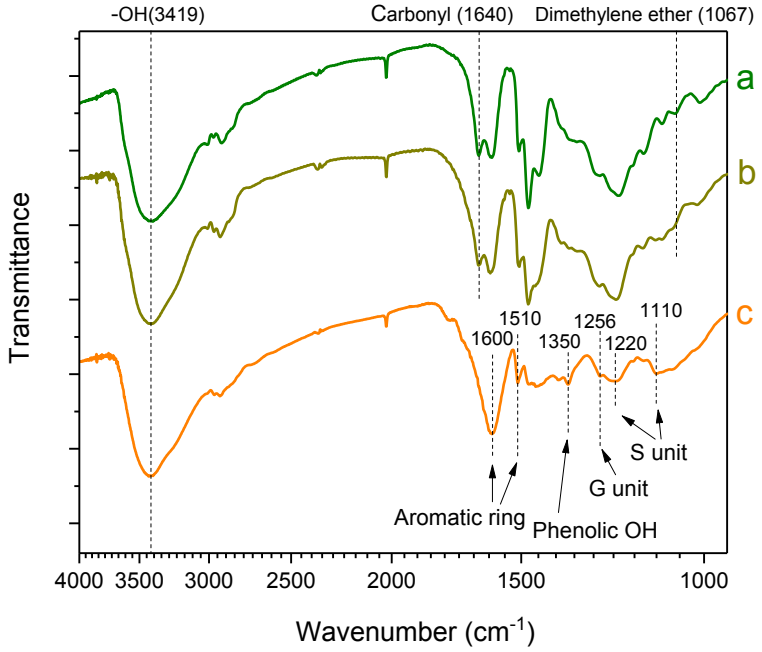

Figure S1 FTIR spectra of PR (a), LPR (b), and the solid substance in the synthesis solution after removal of LPR nanospheres (c).

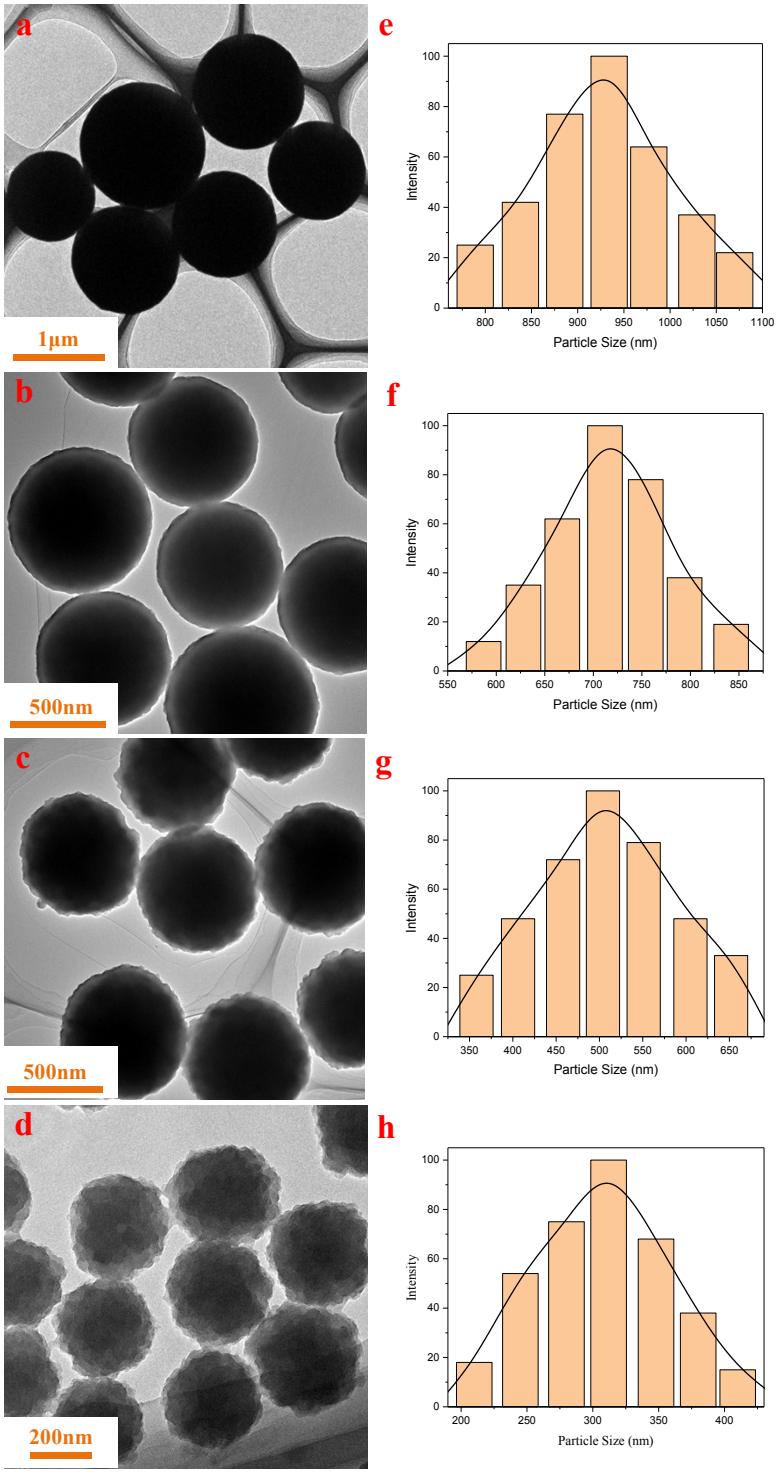

Figure S2 Typical TEM images of LPR spheres: (a) LPR-5%, (b) LPR-10%, (c) LPR-20% and (d) LPR-40%; (e-h) the size distribution histograms of the corresponding LPR spheres.

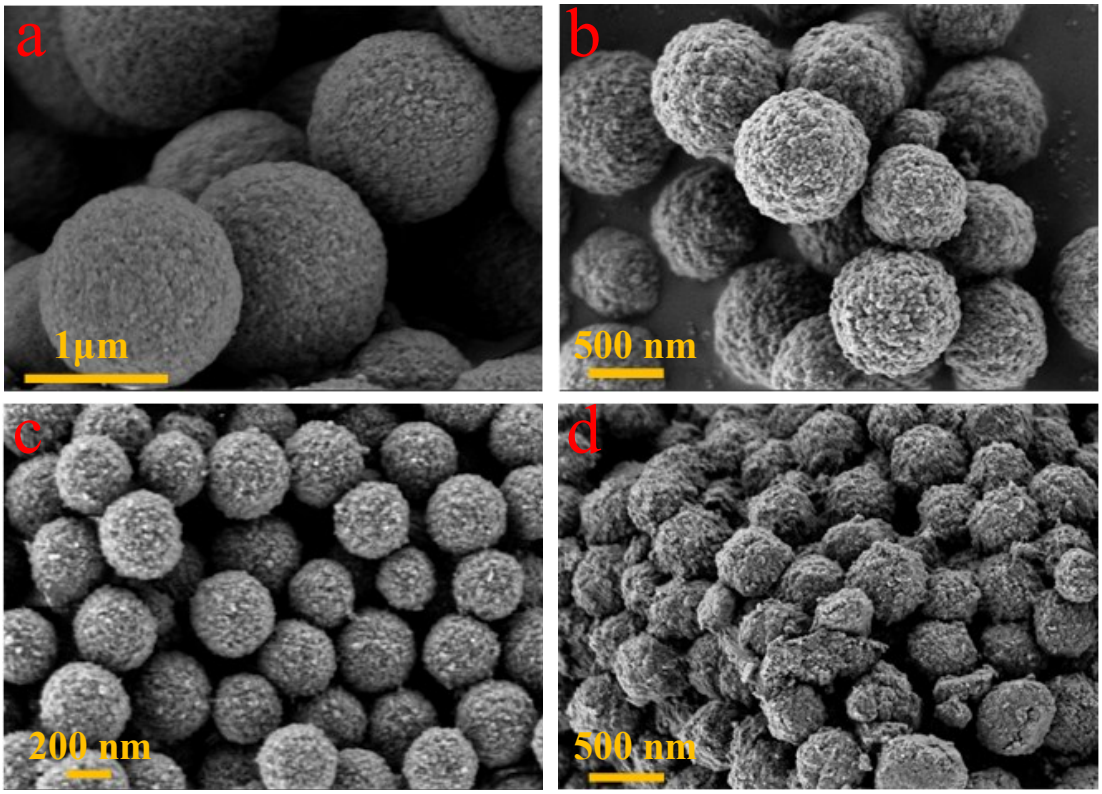

Figure S3 Typical SEM images of LPR spheres prepared using sodium lignosulfonate as the feedstock, (a) LPR-5%; (b) LPR-10%; (c) LPR-20%; (d) LPR-40%.

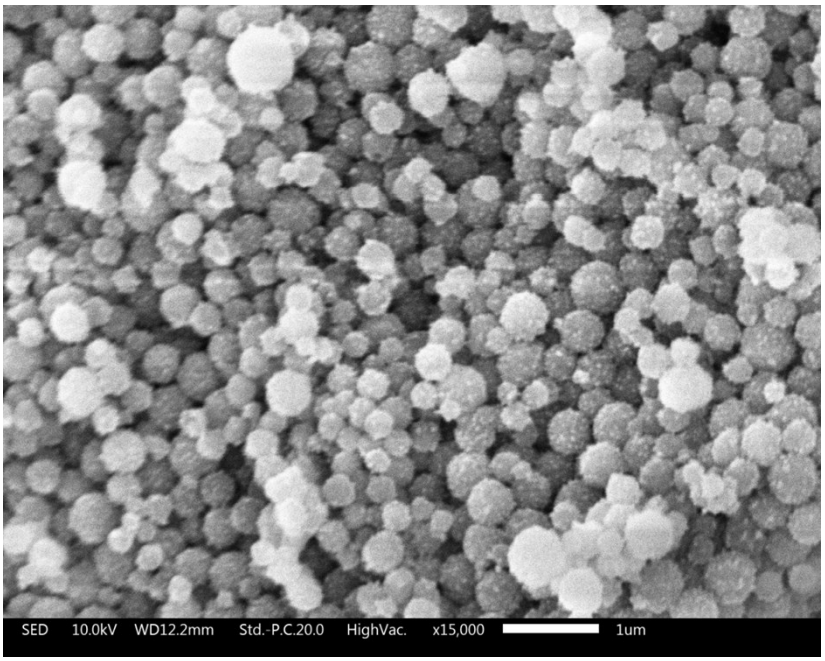

Figure S4 SEM images of LPR@Ag-10 nanocomposites.

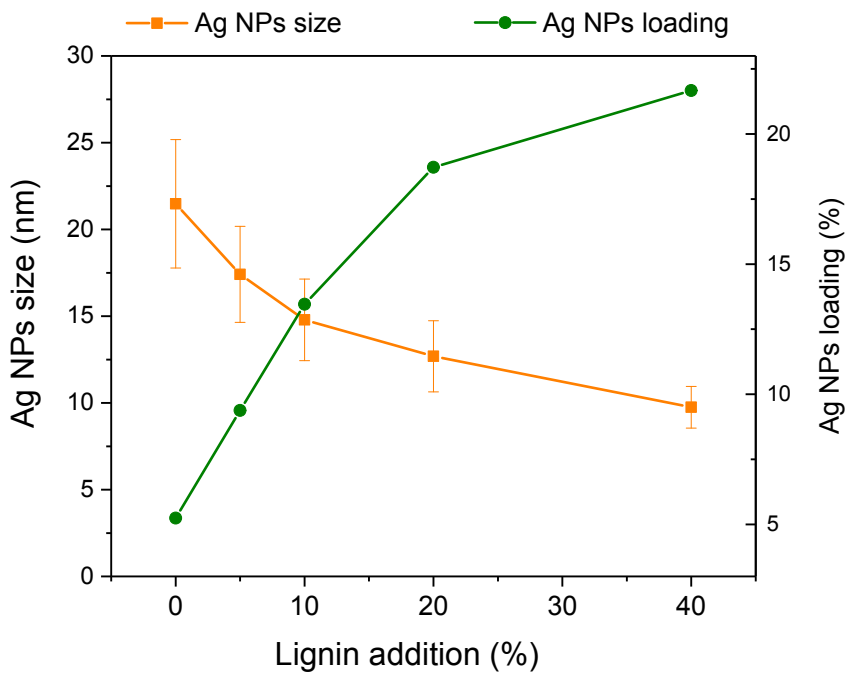

Figure S5 Effects of lignin addition ratios (replacement ratios of phenol by lignin) on the Ag NPs sizes formed on LPR spheres and the Ag NPs loading content.

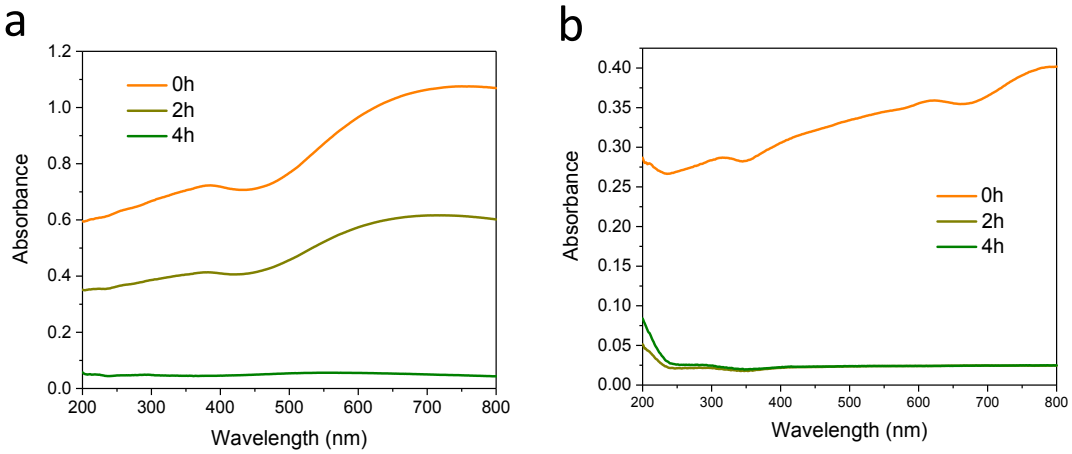

Figure S6 (a) Uv-vis spectra of PR nanospheres dispersed in water for 0, 2, and 4 h; (b) Uv-vis spectra of PR@Ag-10 dispersed in water for 0, 2, and 4 h.

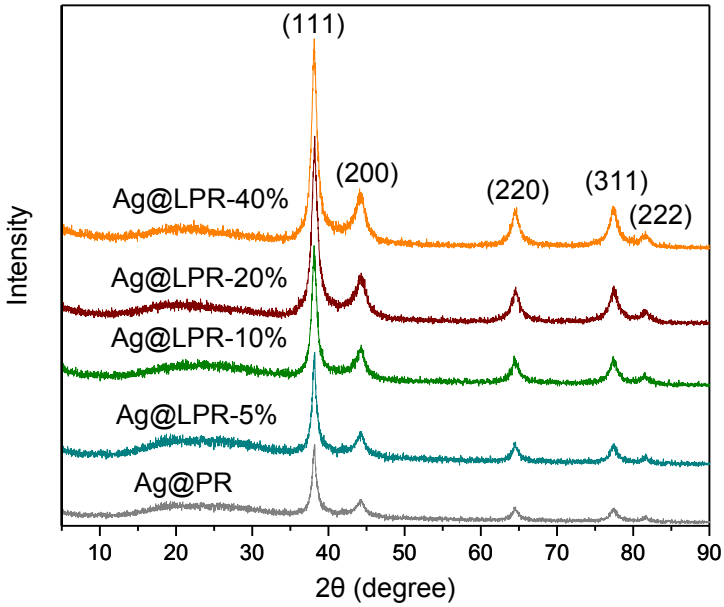

Figure S7 XRD patterns of LPR@Ag composites with different lignin addition ratios.

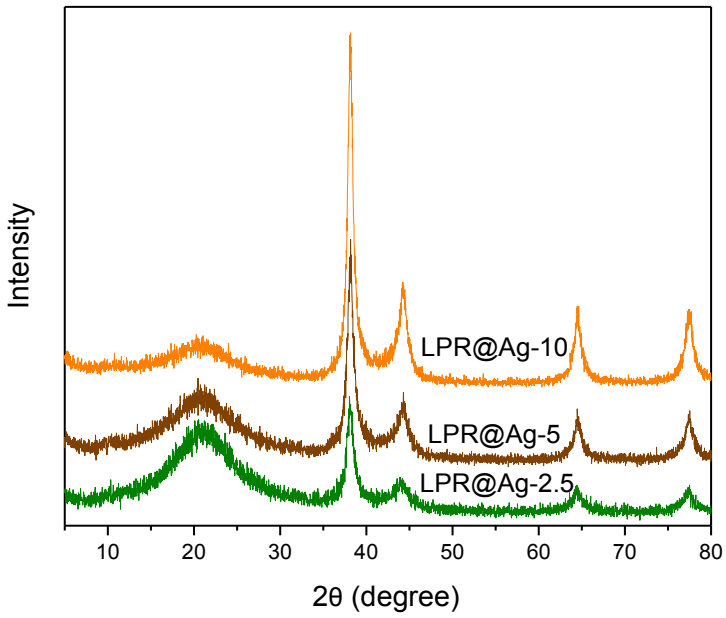

Figure S8 XRD patterns of LPR@Ag-10 nanocomposites (LPR@ Ag-2.5, LPR@ Ag-5, LPR@ Ag-10)

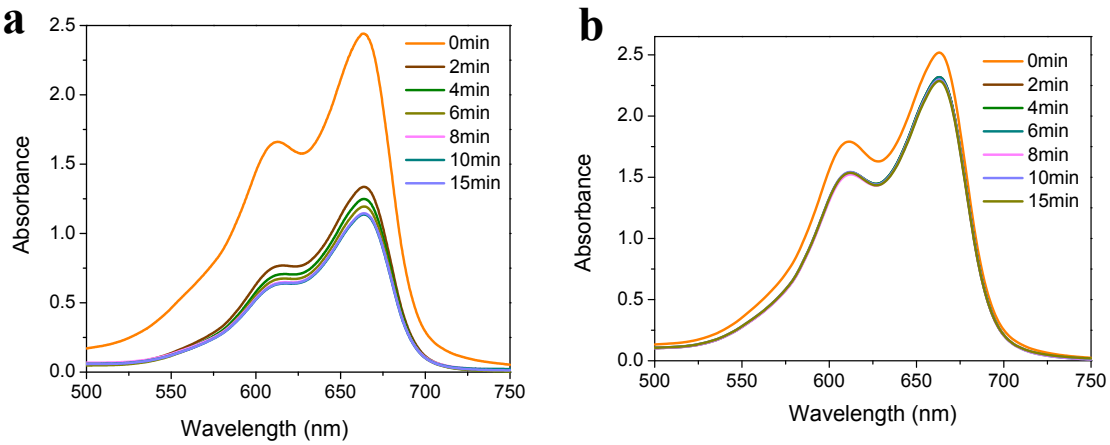

Figure S9 Time-dependent UV-vis spectra for adsorption of methylene blue solution (40 mg/L) by LPR@Ag-10 (c) and PR@Ag-10 (d) without addition of $NaBH_4$.

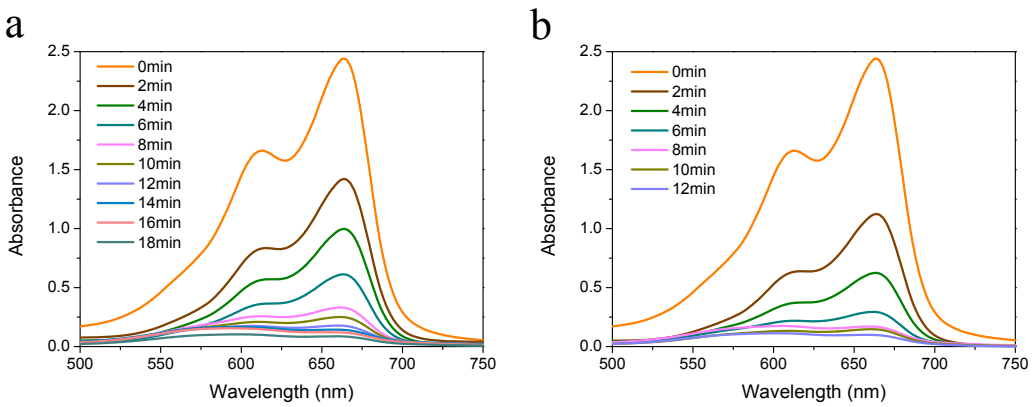

Figure S10 Time-dependent UV−vis spectra for catalytic reduction of methylene blue aqueous solution (40 mg/L) by LPR@Ag-2.5 (a) and LPR@Ag-5 (b).

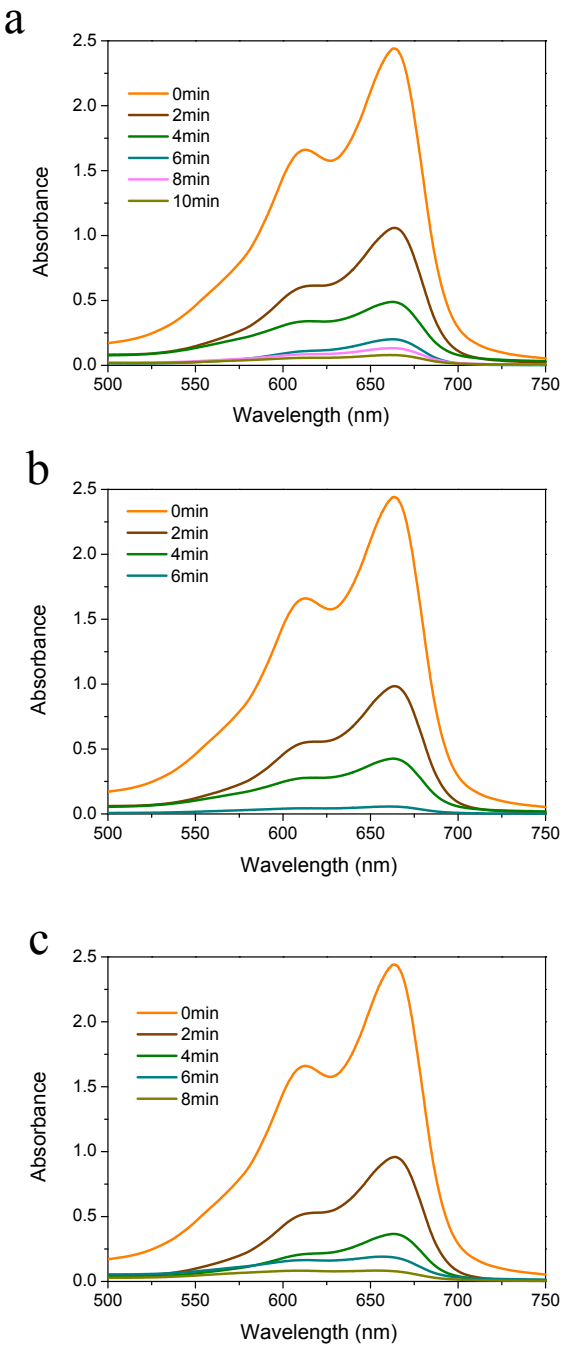

Figure S11 Time-dependent UV−vis spectra for catalytic reduction of methylene blue aqueous solution (40 mg/L) by LPR@Ag-10 nanocomposites at pH=3.0 (a), pH=7.0 (b) and pH=9.0 (c).

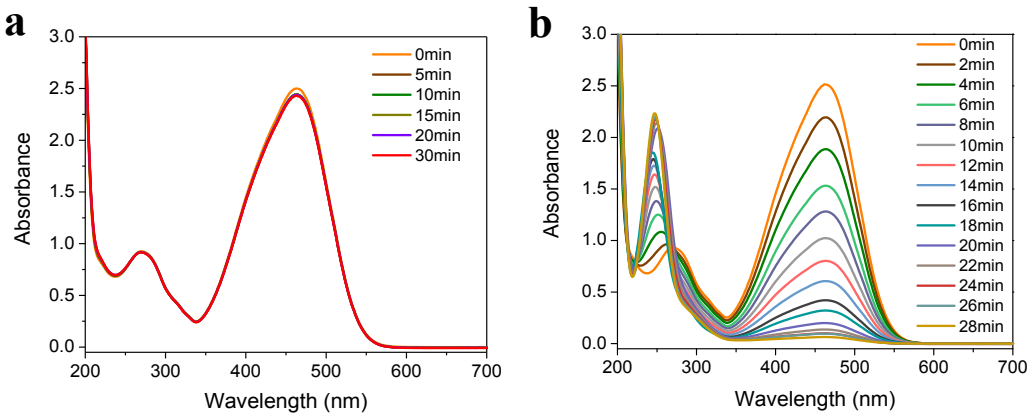

Figure S12 (a) Time-dependent UV-vis spectra for adsorption of methyl orange solution (40 mg/L) by LPR@Ag-10; (b) Time-dependent UV-vis spectra for catalytic reduction of methyl orange solution (40 mg/L) by PR@Ag-10 in the presence of $NaBH_4$.

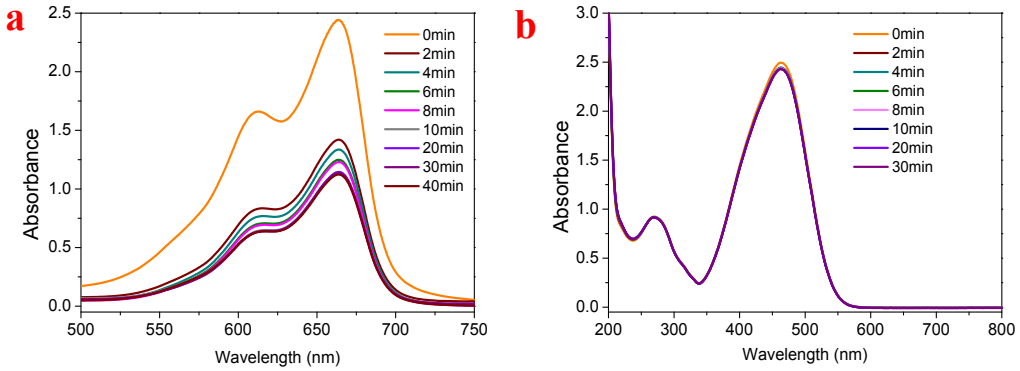

Figure S13 Time-dependent UV-vis spectra of methylene blue solution (40 mg/L) by LPR nanosphere in the presence of $NaBH_4$ (a) and UV-vis spectra of methyl orange aqueous solution (40 mg/L) by LPR nanosphere in the presence of $NaBH_4$ (b).

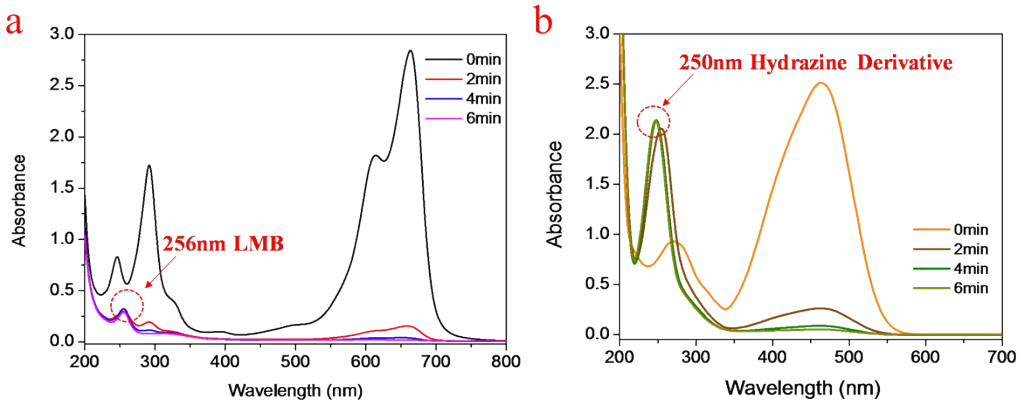

Figure S14 UV-vis spectra for the reduced products of methylene blue (a) and methyl orange (b) by LPR@Ag-10 nanocomposites in the presence of $NaBH_4$.

Table S2 Comparison of catalytic activities of Ag-based catalysts for reduction of methylene blue.

Catalyst	Ag NPs size (nm)	MB (mg/L)	Time (min)	κ_{app} (min^{-1})	Reference
AgNPs-entrapped hydrogel	~20	20	30	-	[2]
Ag/PSNM-3	16.56	9.6	11	0.13	[3]
Fe_3O_4@HA@Ag MNCs	13.25	3.2	20	0.08	[4]
AgNP-agar hydrosol	10.16	32.7	6	0.67	[5]
Multilayer Ag nanoparticles	35–50	6.4	16	0.058	[6]
Fe_3O_4@Polydopamine-Ag	~25	40	9	0.43	[7]
AgNP-starch	18.2±0.97	32.7	10	0.13	[8]
Ag NPs-embedded hybrid microgels	3~6	3.7	28	0.058	[9]
AgNPs@Caulerpa racemosa	25	16	30	0.067	[10]
LPR@Ag-10	10	40	6	0.815	This work

References

[1] G. Wang, X. Liu, J. Zhang, W. Sui, J. Jang, C. Si, One-pot lignin depolymerization and activation by solid acid catalytic phenolation for lightweight phenolic foam preparation, Ind Crops and Prod, 124 (2018) 216-225.

[2] Y. Zheng, A. Wang, Ag nanoparticle-entrapped hydrogel as promising material for catalytic reduction of organic dyes, J Mater Chem, 22 (2012) 16552–16559.

[3] G. Liao, Q. Li, W. Zhao, Q. Pang, H. Gao, Z. Xu, In-situ construction of novel silver nanoparticle decorated polymeric spheres as highly active and stable catalysts for reduction of methylene blue dye, Appl Catal A: Gen, 549 (2018) 102-111.

[4] M. Amir, S. Güner, A. Yıldız, A. Baykal, Magneto-optical and catalytic properties of Fe_3O_4@HA@Ag magnetic nanocomposite, J Magn Magn Mater, 421 (2017) 462-471.

[5] S. Joseph, B. Mathew, Microwave-assisted facile synthesis of silver nanoparticles in aqueous medium and investigation of their catalytic and antibacterial activities, J Mol Liq, 197 (2014) 346-352.

[6] M. Sureshkumar, P.-N. Lee, C.-K. Lee, Stepwise assembly of multimetallic nanoparticles via self-polymerized polydopamine, J Mater Chem, 21 (2011) 12316–12320.

[7] Y. Xie, B. Yan, H. Xu, J. Chen, Q. Liu, Y. Deng, H. Zeng, Highly regenerable mussel-inspired Fe_3O_4@polydopamine-Ag core-shell microspheres as catalyst and adsorbent for methylene blue removal, ACS Appl Mater Interfaces, 6 (2014) 8845-8852.

[8] S. Joseph, B. Mathew, Facile synthesis of silver nanoparticles and their application in dye degradation, Mater Sci Eng B, 195 (2015) 90-97.

[9] Y. Tang, T. Wu, B. Hu, Q. Yang, L. Liu, B. Yu, Y. Ding, S. Ye, Synthesis of thermo- and pH-responsive Ag nanoparticle-embedded hybrid microgels and their catalytic activity in methylene blue reduction, Mater Chem Phys, 149-150 (2015) 460-466.

[10] T.N. Edison, R. Atchudan, C. Kamal, Y.R. Lee, Caulerpa racemosa: a marine green alga for eco-friendly synthesis of silver nanoparticles and its catalytic degradation of methylene blue, Bioprocess Biosyst Eng, 39 (2016) 1401-1408.